Impaired neurotransmission caused by overexpression of α-synuclein in nigral dopamine neurons

Martin Lundblad[1], Mickael Decressac, Bengt Mattsson, and Anders Björklund[1]

Wallenberg Neuroscience Center, Department of Experimental Medical Sciences, Lund University, Lund 221 84, Sweden

This contribution is part of the special series of Inaugural Articles by members of the National Academy of Sciences elected in 2011.

Contributed by Anders Bjorklund, January 13, 2012 (sent for review October 10, 2011)

We used in vivo amperometry to monitor changes in synaptic dopamine (DA) release in the striatum induced by overexpression of human wild-type α-synuclein in nigral DA neurons, induced by injection of an adeno-associated virus type 6 (AAV6)–α-synuclein vector unilaterally into the substantia nigra in adult rats. Impairments in DA release evolved in parallel with the development of degenerative changes in the nigrostriatal axons and terminals. The earliest change, seen 10 d after vector injection, was a marked, ≈50%, reduction in DA reuptake, consistent with an early dysfunction of the DA transporter that developed before any overt signs of axonal damage. At 3 wk, when the first signs of axonal damage were observed, the amount of DA released after a KCl pulse was reduced by 70–80%, and peak DA concentration was delayed, indicating an impaired release mechanism. At later time points, 8–16 wk, overall striatal innervation density was reduced by 60–80% and accompanied by abundant signs of axonal damage in the form of α-synuclein aggregates, axonal swellings, and dystrophic axonal profiles. At this stage DA release and reuptake were profoundly reduced, by 80–90%. The early changes in synaptic DA release induced by overexpression of human α-synuclein support the idea that early predegenerative changes in the handling of DA may initiate, and drive, a progressive degenerative process that hits the axons and terminals first. Synaptic dysfunction and axonopathy would thus be the hallmark of presymptomatic and early-stage Parkinson's disease, followed by neuronal degeneration and cell loss, characteristic of more advanced stages of the disease.

neurodegeneration | synaptic transmission

In Parkinson's disease (PD) damage to axons and axonal terminals is likely to precede any overt dopamine (DA) neuron cell death, suggesting that the disease process may start at the axon terminal level and progress retrogradely to affect the cell bodies. Support of this idea comes from autopsy studies of brains from PD patients, which suggest that the extent of damage to the DA terminals in caudate nucleus and putamen at the time of disease onset is more extensive than the loss of DA neurons in the substantia nigra (see ref. 1 for a recent review). Although genuine longitudinal data are difficult to obtain in human material, available postmortem data indicate that the loss of DA in the caudate nucleus at the time of onset of symptoms is on the order of 70–80%, whereas as much as 70% of the nigral DA cell bodies may still be alive (1–5). Measurement of binding to the vesicular monoamine transporter (VMAT), which is likely to be a good measure of the functional integrity of the DA terminals, has shown severe loss of VMAT in the caudate nucleus early in the disease in some patients (6).

Together, these data suggest that impairments at the terminal/synaptic level may be a prominent feature of presymptomatic and early-stage PD and that impaired DA neurotransmission may contribute to the functional deficits seen also at more advanced stages of the disease. Studies in cell culture point to α-synuclein as a possible mediator of these early changes, including effects on DA synthesis, storage and release (7–9), and vesicular trafficking (9, 10). In vivo studies performed in α-synuclein knockout mice, moreover, have shown that α-synuclein plays a role in the regulation of transmitter storage and release in DA neurons (11–13), suggesting that the synaptic release machinery may be an important target for α-synuclein–induced toxicity.

In the present study we used in vivo amperometry to monitor changes in synaptic DA release in the striatum in rats overexpressing human WT α-synuclein in the nigrostriatal DA neurons, induced by injection of an adeno-associated virus type 6 (AAV6)–α-synuclein vector unilaterally into the substantia nigra. AAV-mediated overexpression of α-synuclein provides an interesting model of PD-like pathology in that the degenerative changes develop progressively over time, from the early signs of axonal damage and α-synuclein aggregation, seen at 2–3 wk after vector injection, followed by neurodegeneration and DA neuron cell loss which develops over the subsequent weeks (14–18). This model offers an opportunity to monitor the functional changes that take place in α-synuclein–overexpressing DA neurons at stages that match the presymptomatic, early, and advanced stages of the human disease.

Results

Changes in striatal DA release were studied at five different time points after vector injection that match progressively more advanced stages of α-synuclein–induced pathology: at 10 d and 3 wk after vector injection, when α-synuclein is fully expressed but before any major cell loss has occurred; at 5 wk, when DA neurodegeneration is well under way; and at 8 and 16 wk, when DA neuron cell loss is complete and the remaining neurons survive long-term in a compromised state, characterized by high levels α-synuclein expression and abundant signs of axonal pathology and loss of terminals (18). Recordings were made bilaterally in urethane-anesthetized rats from electrodes implanted into the center of the caudate putamen (Fig. 1*A*). With this design, the noninjected intact side could be used as a reference in all measurements. The control rats received an intranigral injection of the control AAV-GFP vector and were analyzed at 10 d, 3 wk, or 5 wk after injection. The extracellular DA concentration was monitored using chronoamperometry (1-Hz recordings). DA release was evoked by short pulse (<1 s) pressure ejection of a fixed amount of KCl adjacent to the recording electrode. Four measures were taken from the resulting DA release curves, as indicated in Fig. 1*B*: *peak amplitude*, reflecting the maximal extracellular concentration of DA; *reuptake rate*, reflecting the rate by which the released DA was eliminated from the extracellular space; *linear rise rate*, which is determined by the speed by which K^+-evoked DA is released from the DA terminals into the extracellular space; and *area under the curve* (AUC), which is a measure of the total amount of DA available to act on the postsynaptic receptors over time.

Author contributions: M.L., M.D., and A.B. designed research; M.L., M.D., and B.M. performed research; M.L., M.D., and A.B. analyzed data; and A.B. wrote the paper.

The authors declare no conflict of interest.

[1]To whom correspondence may be addressed. E-mail: Anders.Bjorklund@med.lu.se or Martin.Lundblad@med.lu.se.

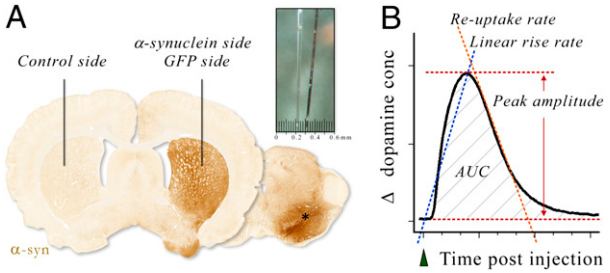

Fig. 1. (*A*) Coronal sections through the forebrain and midbrain, stained with a human-specific α-synuclein antibody, from a rat that received a unilateral 3-μL injection of the AAV–α-synuclein vector just above the substantia nigra (asterisk) 10 d erlier. Human WT α-synuclein derived from the vector is expressed in the DA neurons of the substantia nigra and distributed throughout the ipsilateral caudate-putamen. *Inset*: Electrode/micropipette assembly used for recording; the vertical lines mark the bilateral recording sites. (*B*) The four measurement parameters—peak amplitude, linear rise rate, reuptake rate, and AUC—were calculated from the DA release curve, as indicated.

Time-Dependent Effects on K^+-Evoked DA Release. As illustrated in Fig. 2, we observed a significant change in the shape of the DA release curve already at 10 d after injection: the peak was significantly broader and shifted to the right (Fig. 2, *Left*). Further analysis revealed a significant reduction in the reuptake rate (Fig. 3*B*; two-factor ANOVA, time effect $P = 0.58$, side effect $P < 0.0001$, time and group interaction $P < 0.0001$, Student t test for 10-d time point, $P < 0.05$), whereas the peak amplitude was unaffected (Fig. 3*A*; two-factor ANOVA and Student t test, $P > 0.05$). The linear rise rate seemed to be reduced in several of the animals at 10 d, but this did not reach significance in the group as a whole (Fig. 3*C*). From 3 wk onward, DA release amplitude was markedly reduced at all time points (two-factor ANOVA, time effect $P = 0.0213$, group effect $P < 0.0001$, 3–16 wk α-synuclein vs. control side; Student t test, $P < 0.05$). At the early time points, 3 and 5 wk in particular, the peaks tended to be broader and shifted to the right (red traces in Fig. 2). The peak amplitude was reduced by 70–80% (average 83%) at 3 and 5 wk, and 80–90% (average 93%) at 8 and 16 wk, compared with both the intact control side and the injected side in the AAV-GFP–treated animals (Fig. 3*A*). Consistent with the change in the shape of the release curve, both the reuptake rate (Fig. 3*B*) and the linear rise rate (Fig. 3*C*) were significantly reduced, ranging from 75% to 95% at time points from 3 wk to 16 wk (two-factor ANOVA and Student t test, $P < 0.05$). Total DA release, measured as the AUC (Fig. 1), was similarly affected (Fig. 3*D*; two-factor ANOVA, time effect $P = 0.87$, group effect $P < 0.0001$, time and group interaction $P = 0.0014$; Student t test, $P < 0.05$ for 3–16 wk time points vs. control side) and followed closely the changes seen in peak amplitude (Fig. 3*A*).

Dose Dependency. The changes summarized in Figs. 2 and 3 were obtained in rats injected with a vector containing the woodchuck hepatitis virus posttranscriptional regulatory element (WPRE) enhancer element. As reported in the parallel study (18) the α-synuclein expression obtained with this vector construct is high, approximately four- to fivefold above the endogenous α-synuclein level. To explore whether there is a critical threshold of α-synuclein overexpression for synaptic dysfunction to develop, we added a group of rats that received an identical intranigral injection of the AAV–α-synuclein vector lacking the WPRE enhancer, known to result in a lower level of expression, estimated at two- to threefold above the endogenous one (18). As illustrated in Fig. 4, α-synuclein expressed at this level resulted in a reduction of striatal DA release by approximately 20–30%, as assessed at 3–5 wk after vector injection, suggesting that the impairment indeed was dose dependent. This reduction, which was approximately half of that seen in the animals treated with the WPRE-containing vector (Fig. 3), reached significance for two of the four parameters, amplitude (Fig. 4*A*) and DA reuptake rate (Fig. 4*B*).

Elimination of Exogenous DA from the Extracellular Space. The data obtained at 10 d after vector injection suggested that the shift in the release curve seen at this early time point was mainly due to reduced elimination of DA from the extracellular space. To confirm that this indeed was the case, we performed an experiment in a separate group of animals, treated 10 d earlier with the WPRE-containing vector, whereby a pulse of DA was injected adjacent to the electrode tip, and the extracellular concentration of DA was monitored over the subsequent 200 s. As shown in Fig. 5, the elimination of DA was considerably slower on the α-synuclein–overexpressing side, and the DA reuptake rate, calculated as indicated in Fig. 5*A*, was reduced by 61% compared with the contralateral intact striatum (paired t test, $P = 0.0069$).

DA Release in the Presence of Reuptake Blockade. To obtain a more direct measure of tonic DA release from the α-synuclein–overexpressing striatal terminals, we performed a series of measurements of the change of basal extracellular levels of DA, in the absence of any added KCl, which is made possible by the use of local application of a DA reuptake blocker, nomifensine. These

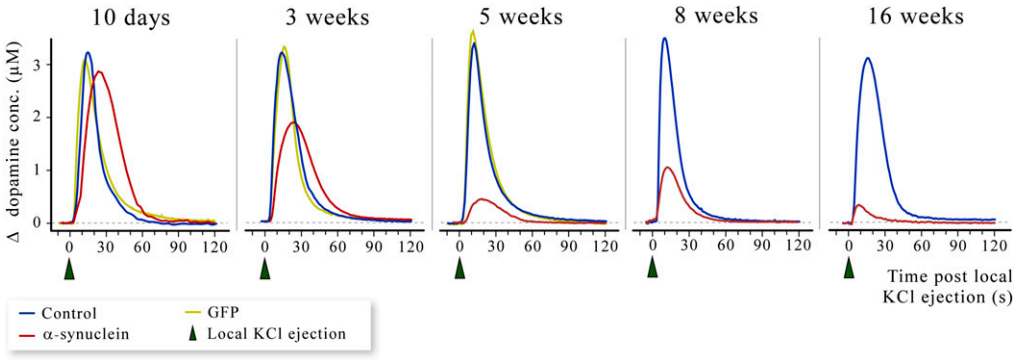

Fig. 2. Traces showing the change in extracellular DA concentration recorded simultaneously from the noninjected control side (blue) and the AAV–α-synuclein injected side (red), elicited by the KCl pulse, at four time points after vector injection. Note the pronounced broadening of the DA release curve seen already at the 10-d time point and the progressive reduction in the peak amplitude. Yellow traces show DA release recorded from animals injected with the AAV-GFP control vector.

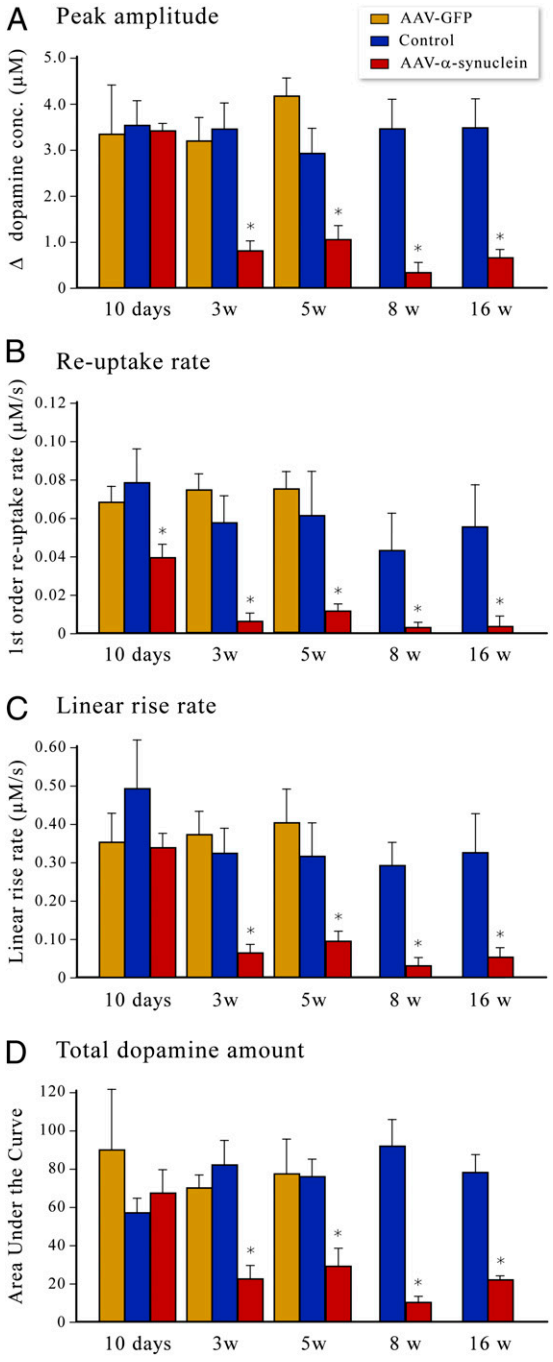

Fig. 3. Changes in (*A*) peak amplitude, (*B*) reuptake rate, (*C*) linear rise rate, and (*D*) AUC, recorded simultaneously at the five time points from the AAV–α-synuclein injected side (red bars) and the noninjected control side (blue bars). A significant reduction in the DA reuptake rate is seen already at 10 d. Yellow bars show recordings from separate groups of animals injected with the AAV-GFP control vector. *$P < 0.05$; one-way ANOVA followed by Student *t* test.

measurements were performed at four time points: 10 d and 3, 5, and 8 wk after AAV–α-synuclein (+WPRE) injection.

Local injection of nomifensine resulted in a sharp rise in extracellular DA concentration, reaching a peak level within a few minutes, followed by a slow decline over the subsequent 20–30 min, reflecting the elimination of DA by enzymatic degradation and diffusion (Fig. 6*B*). The results show an interesting, progressive decline in DA release, measured as the peak amplitude, over the 8-wk period on the α-synuclein–overexpressiong side (Fig. 6*A*; two-factor ANOVA, time effect $P = 0.0007$, group effect $P = 0.0001$, time and group interaction $P = 0.89$; Student *t* test, $P < 0.05$ at 3–8 wk vs. control side). Consistent with the K^+-evoked release data (Fig. 3*C*), there was an overall trend toward reduced tonic release, by approximately 20%, at 10 d, which became progressively more pronounced at 3 wk (−50%), 5 wk (−70%), and 8 wk (−80%).

Histology. Analysis of the immunostained sections confirmed that the vector injections were well placed and that human α-synuclein and GFP was well expressed in the nigral DA neurons and their axons innervating the head of the caudate-putamen on the injected side (Fig. 1*A*). The placement of the amperometry electrodes in the center of the head of the caudate-putamen was confirmed. Densitometry performed on the tyrosine hydroxylase (TH) immunostained sections showed a progressive loss of TH-positive terminals in the striatum, starting at 3 wk after vector injection and reaching 60% loss at 8 wk and 80% loss at 16 wk (Fig. 7*L*). The first morphological changes appeared between 10 d, when the innervation appeared completely normal (Fig. 7 *A* and *E*), and 3 wk, when single, scattered distorted TH- and α-synuclein–positive axonal profiles appeared (Fig. 7 *B* and *F*). At later time points, 8 wk (Fig. 7 *C* and *G*) and 16 wk (Fig. 7 *D* and *H*), the overall density of TH- and α-synuclein–positive axons and terminal was progressively reduced, and many of the remaining terminals showed signs of damage, expressed as TH- and α-synuclein–containing axonal swellings (arrowheads in Fig. 7), some of them with the appearance of large end-bulbs (arrows). Analysis at higher power in the microscope revealed that these swellings contained aggregates of spherical, α-synuclein–positive inclusions (see, e.g., Fig. 7 *G* and *H*) and that some of them stained positively for VMAT-2 (Fig. 7 *I–K*), suggesting that the α-synuclein–containing aggregates had incorporated the VMAT transporter.

Immunohistochemistry for DA transporter (DAT) and VMAT-2 showed that the expression of these two proteins was maintained at normal levels in the individual terminals at both 10 d and 3 wk (Fig. 8 *A*, *B*, *D*, and *E*). At longer time points, the swollen, dystrophic axons and terminals stained positively for VMAT-2 (arrow and arrowheads in Fig. 8*F*). DAT, by contrast, was expressed at seemingly normal levels in the remaining terminals, but not in the swollen, dystrophic axonal profiles (Fig. 8*C*).

In contrast to the results obtained with the WPRE-containing vector (above), the animals that received injections of the vector lacking the WPRE enhancer element showed limited loss of TH-positive axons and cells at 3–5 wk postinjection, which is consistent with the results obtained with the same vector in the parallel report (18).

Discussion

The results revealed marked changes in DA neurotransmission already at 10 d and 3 wk after vector injection, before any major DA neuron cell loss has occurred. The earliest change, seen at 10 d, was a reduction in DA reuptake rate, which resulted in a broadening of the DA release curve. The rate of elimination of extracellular DA (delivered as a local injection) was reduced by approximately 60%, suggesting that the function of DAT was markedly impaired already at this stage, before any overt signs of neuronal cell loss have occurred. At 3 wk the first signs of axonal damage were observed in the form of α-synuclein–filled axonal swellings and dystrophic terminals that stained positively for both TH and VMAT-2. The overall reduction in the striatal TH-positive innervation was minor at this point, only approximately 20%. At this stage, all parameters of DA release—peak amplitude, reuptake rate, linear rise rate, and AUC—were dramatically reduced, pointing to an impairment not only in DA reuptake but also in the mechanism of release. This was reflected

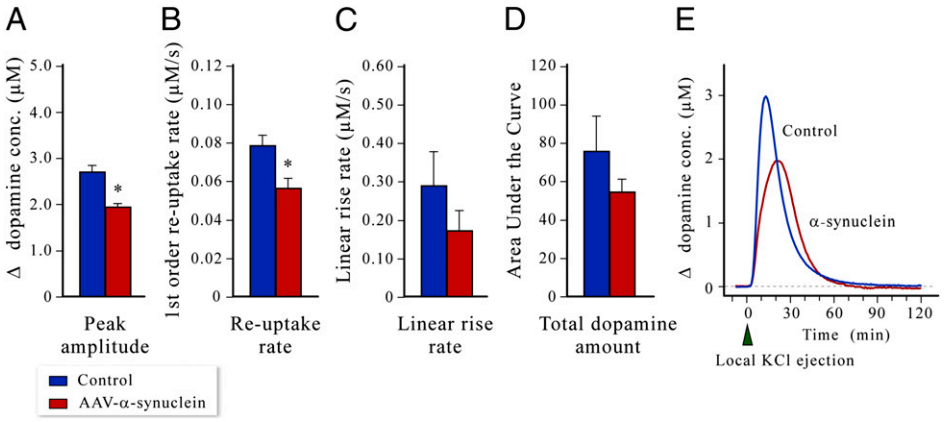

Fig. 4. Changes in (*A*) peak amplitude, (*B*) reuptake rate, (*C*) linear rise rate, and (*D*) AUC, induced by the WPRE-lacking AAV–α-synuclein vector ($n = 3$). As in Fig. 3, the recordings were made simultaneously from the AAV–α-synuclein injected side (red bars) and the noninjected control side (blue bars). (*E*) Actual traces from the two sides in one of the recorded rats. *P < 0.05; Student *t* test.

in a 70–80% reduction in peak amplitude and rate of DA release, as well as a 50% reduction in the amount of DA accumulating extracellularly after blockade of DAT by local injection of nomifensine.

These data are consistent with previous studies showing that the synuclein family of proteins are likely to play a role both in normal physiological neurotransmitter release (11, 12, 19, 20) and in the regulation of transporter function (21, 22). In vitro studies have shown that overexpression of α-synuclein inhibits the release of catecholamines from adrenal chromaffin and PC12 cells, probably owing to a reduced pool of readily releasable vesicles (9). Similarly, Nemani et al. (10) have reported impairment of transmitter release, due to a reduction in the size of the synaptic vesicle recycling pool, in hippocampal and dopaminergic neurons expressing human WT α-synuclein at levels two- to threefold above normal. Our data are also in line with the observations of Chung et al. (17) in the AAV–α-synuclein model, showing significant changes in the levels of proteins involved in synaptic transmission and axonal transport as early as 4 wk after AAV–α-synuclein injection.

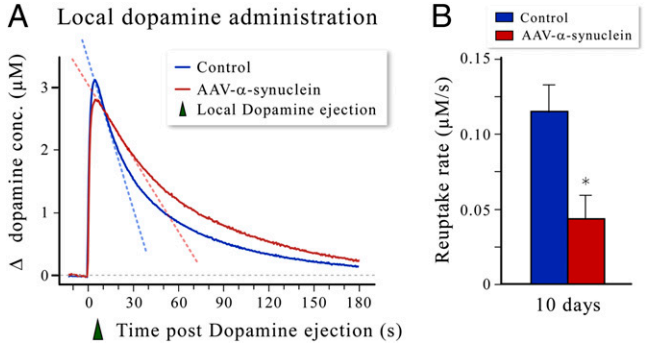

Fig. 5. Changes in DA reuptake were studied, at 10 d after AAV–α-synuclein injection, after local injection of DA. (*A*) A pulse of DA was injected adjacent to the electrode tip, and the extracellular concentration of DA was monitored over the subsequent 200 s on the AAV–α-synuclein injected side (red) and the noninjected control side (blue). As shown in *B*, the elimination of extracellular DA was considerably slower on the α-synuclein–overexpressing side (red bar; $n = 4$), and the DA reuptake rate, calculated as indicated by the dashed lines in *A*, was reduced by approximately 60% compared with the contralateral intact striatum (blue bar; $n = 4$). *$P < 0.05$; one-way ANOVA followed by Student *t* test.

Studies in α-synuclein–overexpressing transgenic mice have so far failed to replicate the detrimental effects seen in cell culture models (23, 24). The results obtained by Yavich et al. in 2005 (23) by in vivo voltammetry, performed in transgenic mice expressing A30P-mutated human α-synuclein, showed no effect on either release or reuptake of DA after electrical stimulation of the nigrostriatal pathway, although the slower rate of decline seen after repeated stimulations was interpreted as a reduced DA storage pool in the transgenic animals. The present results suggest that the detrimental effect of α-synuclein on synaptic

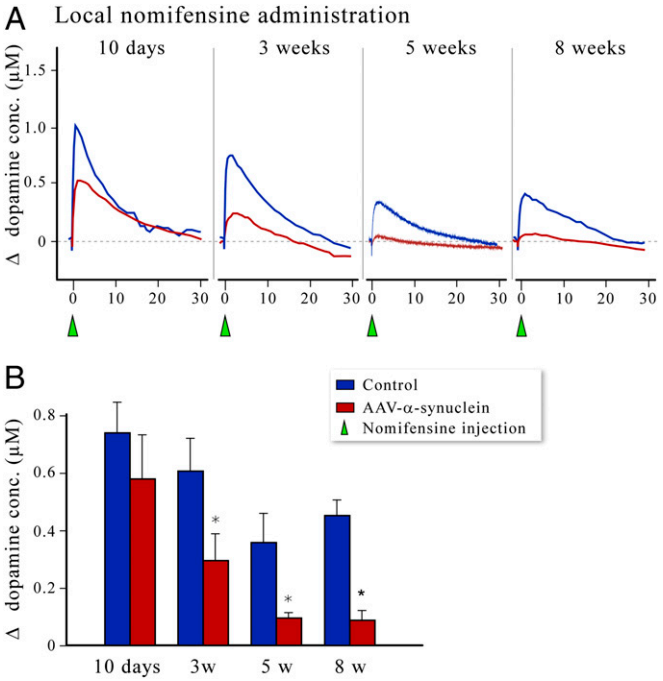

Fig. 6. (*A*) Traces showing the change in extracellular DA concentration on the noninjected control side (blue) and the AAV–α-synuclein injected side (red), elicited by local application of the DA reuptake blocker nomifensine, at four time points after vector injection. (*B*) From 3 wk, onward, there was a significant reduction in the peak amplitude on the AAV–α-synuclein injected side (red bars), compared with the simultaneous recording on the noninjected control side (blue bars), signifying an impaired DA release machinery ($n = 4$ per group). *$P < 0.05$; one-way ANOVA followed by Student *t* test.

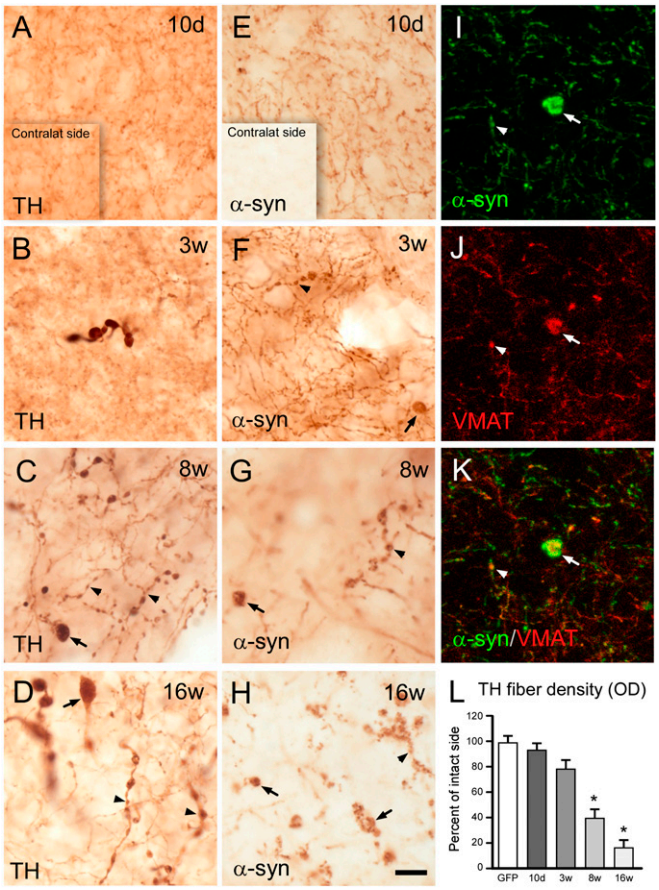

Fig. 7. Changes in the striatal DA terminal network induced by overexpression of human WT α-synuclein, as observed in sections stained for TH (*A–D*) and human α-synuclein (*E–H*). The first pathological changes, observed as scattered swollen dystrophic axonal segments, appeared at 3 wk after vector injection (*B* and *F*). At 8 wk (*C* and *G*) and 16 wk (*D* and *H*) the overall density of TH- and α-synuclein–positive axons and terminal were markedly reduced, and many of the remaining terminals showed signs of damage, expressed as TH- and α-synuclein–containing axonal swellings (arrowheads), some of them with the appearance of large end-bulbs (arrows). Some of these α-synuclein–positive axonal swellings stained positively for VMAT-2 (*I–K*). (*L*) Progressive decline in striatal TH immunorectivity on the vector-injected side, as measured by densitometry (n = 4–6 per group). *$P < 0.05$; one-way ANOVA followed by Student t test. (Scale bar, 10 μm.)

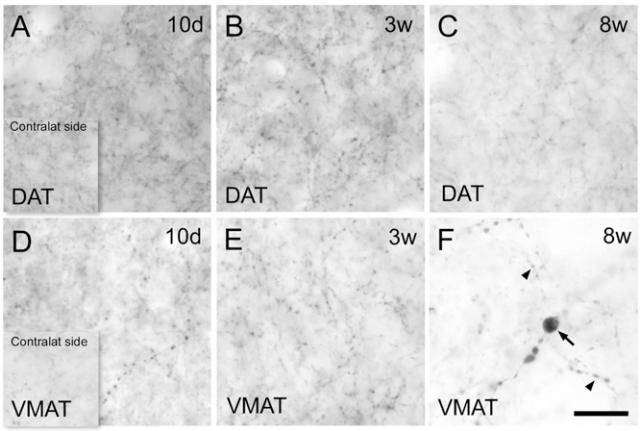

Fig. 8. Sections stained for DAT (*A–C*) and VMAT-2 (*D–F*) showed that the expression of DAT and the vesicular transporter, in individual striatal DA terminals, was maintained at normal levels at both 10 d (*A* and *D*) and 3 wk (*B* and *E*) after AAV–α-synuclein injection. (*F*) At 8 wk, the swollen, dystrophic axons and terminals stained positively for VMAT-2. (*C*) DAT, by contrast, was expressed at seemingly normal levels in the remaining terminals but not in axons with swollen, dystrophic profiles. (Scale bar, 10 μm.)

function is dose-dependent and that the high α-synuclein expression levels obtained with AAV–α-synuclein vector used here, estimated at two- to threefold above the endogenous level with the vector lacking WPRE and at four- to fivefold with the WPRE-containing vector (18), may be needed to induce significant changes in striatal DA release and reuptake in vivo. Such high levels may not have been achieved in the nigrostriatal DA neurons in the transgenic mice studied to date.

The earliest change seen on the AAV–α-synuclein transduced side was the reduction in DA reuptake, which was reduced by approximately 50% already at 10 d after vector injection, before the emergence of any degenerative changes. At 3 wk the reduction in DA reuptake, approximately 80–90%, exceeded by far the extent of loss of striatal TH-positive innervation, approximately 20%, as judged by TH immunostaining. Interestingly, the expression of the DAT protein in axons and terminals was maintained in the surviving DA innervation at all time points, suggesting that the effect seen on DA reuptake is due to impaired function, rather than an actual loss, of the DAT protein. This is in line with previous observations made in α-synuclein–overexpressing cell lines, showing that increased levels of α-synuclein induce a dose-dependent reduction in DAT function and that this effect is mediated via an increased trafficking of the transporter away from the cell surface without any change in the DAT expression level (21, 22) On the basis of these in vitro studies it seems likely that the impairment in DA reuptake seen here is due to an internalization of DAT leading to a reduced capacity for transport of DA across the membrane.

DAT is an important modulator of DA neurotransmission, through its ability to regulate the concentration and the spread of extracellular DA at the synapse. At the early stages after vector injection the reduction in DA reuptake induced by increased levels of α-synuclein was accompanied by a marked broadening of the release curve, indicating that the released DA survived longer in the extracellular space. This provides an interesting compensatory mechanism by which the affected terminals can maintain functional extracellular levels of DA and activation of postsynaptic DA receptors, also at stages when the release mechanism of the remaining terminals is impaired. The reduction in DA release may thus be compensated for, in part, by the slower elimination of released DA from the extracellular space. This compensatory mechanism may explain the delay in appearance of behavioral impairments in the AAV–α-synuclein treated animals, which become prominent only at 8–16 wk after vector injection (18).

An intriguing finding of the present study is that the impairments in DA release evolved in parallel with the development of degenerative changes in the nigrostriatal axons and terminals, appearing as α-synuclein- and TH-filled axonal swellings and truncated, dystrophic axonal profiles. This is consistent with the idea that impaired DA storage may play a role in the initiation of the degenerative changes linked to α-synuclein toxicity (7, 25). There are experimental data to suggest that α-synuclein can act as a regulator of vesicle recycling at the presynaptic terminal and that a decreased storage capacity in combination with permeabilization of storage vesicles by toxic species of α-synuclein will lead to increased cytoplasmic levels of DA (7, 21, 26). Increased cytoplasmic DA, in turn, will lead to free radical damage and will also interact with α-synuclein to form toxic forms of the molecule (27, 28), thus initiating a vicious circle that is detrimental to the cell.

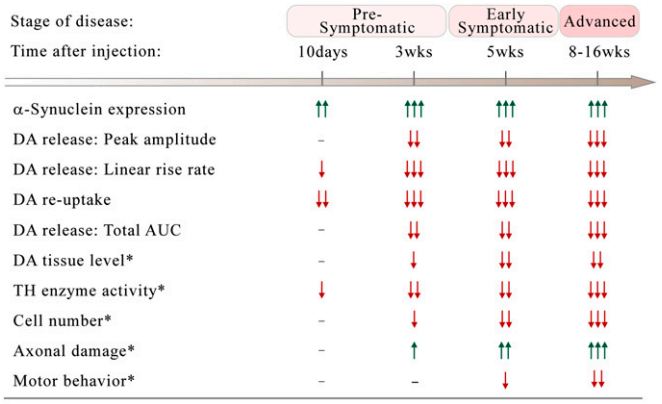

* *Data from ref. 18*

Fig. 9. The changes that develop in the striatal dopaminergic innervation over time make it possible to define distinct stages of damage and impairment that correspond to the presymptomatic, early symptomatic, and advanced stages of the human disease. The presymptomatic stage, which develops within the first 3 wk after AAV–α-synuclein injection, is characterized by impaired transmitter release and reuptake at the synaptic level, and early signs of axonal damage, but without any major cell loss. The first signs of behavioral impairments, representing an early symptomatic stage, are seen at 5 wk after vector injection. At this stage neurodegeneration is well under way, accompanied by a partial loss of the striatal dopaminergic innervation, more abundant signs of axonal damage, and a reduction in striatal DA levels. The advanced stage, seen at 8–16 wk, when degeneration of the nigral DA neurons is complete, is characterized by severe loss of TH-positive terminals in the striatum, accompanied by significant impairment in motor behavior. Remaining axons and terminals in the striatum show signs of ongoing pathology, including large α-synuclein-, TH-, and VMAT-2–containing dystrophic axonal profiles. Our amperometry data suggest that this remaining innervation is dysfunctional but that the severe reduction of DA reuptake, which far exceeds the magnitude of loss of TH-positive terminals, will help to maintain DA neurotransmission at a functional level and thus delay the appearance of more profound motor deficits.

In this scenario, the early predegenerative changes in DA release seen in the AAV–α-synuclein model would represent an early defect in the handling of synaptic DA that interacts with α-synuclein to initiate, and drive, a progressive degenerative process that hits the axons and terminals first. Synaptic dysfunction leading to axonopathy would thus be the hallmark of presymptomatic and early-stage PD, followed by neuronal degeneration and cell loss, characteristic of the symptomatic and more advanced stages of PD. The sequence of degenerative changes seen in the AAV–α-synuclein treated animals, as summarized in Fig. 9, provides a model of progressive PD. The changes seen during the first 3 wk after vector injection, which take place before any behavioral impairment is detectable, represent a presymptomatic stage, characterized by impaired transmitter release and reuptake at the synaptic level, a 40–60% reduction in striatal TH enzyme activity, and early signs of axonal damage, but without any major cell loss (17, 18). The first signs of behavioral impairments, representing an early symptomatic stage, are seen at 5 wk after vector injection. At this stage neurodegeneration is well under way, accompanied by a partial loss of the striatal dopaminergic innervation, more abundant signs of axonal damage, and a reduction in striatal DA levels. At 8–16 wk, the degeneration of DA neurons in the SN and the loss of TH-positive innervation in the striatum are complete and accompanied by a significant impairment in both drug-induced and spontaneous motor behavior. Remaining DA neurons survive despite that the expression of the vector-derived α-synuclein is maintained at a high level, partly in the form of inclusions and aggregates, and most of the remaining axons and terminals in the striatum show signs of ongoing pathology, including large α-synuclein and TH/VMAT-2–containing dystrophic axonal profiles. Our amperometry data suggest that this remaining innervation is dysfunctional but that the severe reduction of DA reuptake, which far exceeds the magnitude of loss of TH-positive terminals in the recorded areas, may provide a compensatory mechanism that will help to maintain DA neurotransmission at a functional level and thus delay the appearance of more profound motor deficits.

Materials and Methods

Animals and Surgery. The animals used in the present experiments were part of a larger study designed to investigate the time-dependent degenerative changes induced by AAV-mediated overexpression of WT human α-synuclein (18), thus using the same vectors and surgical procedures as described in this article. The study was performed on adult female Sprague-Dawley rats, 225–250 g at the time of surgery, housed two to three per cage with ad libitum access to food and water during a 12-h light/dark cycle. All procedures were conducted in accordance with guidelines set by the Ethical Committee for the Use of Laboratory Animals in the Lund-Malmö region and the European Ethical Committee (86/609 EEC). The stereotaxic surgery was performed under general anesthesia using a 20:1 mixture of fentanylcitrate (Fentanyl) and medetomidine hypochloride (Domitor) (Apoteksbolaget) injected i.p.

The vectors were of the AAV6 serotype and produced as described earlier (18). The expression of the transgenes (human WT α-synuclein and GFP) were driven by the synapsin-1 promoter and enhanced using WPRE. Genome copy titers, as determined by real-time quantitative PCR, were 3.7×10^{12} and 2.5×10^{12} genome copies/mL for the AAV6–α-synuclein and the AAV6-GFP vector, respectively. In a separate group of three rats we used a vector lacking the WPRE sequence (AAV6–CBA–α-synuclein), as detailed in the parallel report (18). Dilution of the batches was performed so that an equivalent number of genome copies (3.1×10^8 gc/3 μL) was injected in each animal.

The injections were made unilaterally on the right side, above the substantia nigra. Three microliters of the AAV6–α-synuclein and AAV6-GFP vector solutions were infused at a rate of 0.2 μL/min at the following coordinates (flat skull position): anteroposterior, −5.3 mm; mediolateral, −1.7 mm; dorsoventral, −7.2 mm below dural surface as calculated relative to bregma according to the stereotaxic atlas of Paxinos and Watson (29). The needle was left in place for an additional 3 min before it was slowly retracted.

Electrochemical Detection. High-speed chronoamperometric measurements (5 Hz) of extracellular DA levels were performed using a Pentium-IV microcomputer-controlled instrument (FAST-16; Quanteon) as previously described (30). Briefly, a square wave potential was applied (+0.55 V; resting 0.0 V vs. Ag/AgCl reference), and the resulting oxidation and subsequent reduction currents from the microelectrodes were integrated during the final 80% of each 100-ms pulse. Both oxidation and reduction currents were continually recorded and integrated over 1 s.

The electrochemical recording electrodes (Quanteon) consisted of single carbon-fiber electrodes, sealed in a glass capillary (fiber diameter 30 μm; exposed length 120–150 μm) coated at high temperature with Nafion (three coats at 200 °C for 5 min; Sigma Aldrich). Before coating was applied, the electrodes were dried for 5 min at 200 °C. Nafion coating was applied to prevent detection of anionic substances and thus increase the sensitivity for DA. The electrode sensitivity and linearity were determined by generating calibration curves in 0.1 M PBS solutions (pH 7.4) at room temperature for each recording electrode. Electrode responses were regarded as linear for 2-μM increments of DA when $r2 > 0.997$. The electrodes showed high sensitivity to DA but were insensitive to ascorbic acid, with an average selectively ratio of DA to ascorbic acid of 2,060:1 ($n = 50$). Limit of detection, defined as signal-to-noise ratio of 3:1, was 0.0069 ± 0.0013 μM.

The electrodes were mounted together with two glass micropipettes with outer tip diameters of 10–15 μm using sticky wax (Kerr Nordic). The distance between the electrode and micropipettes was 90–110 μm. The micropipette was filled with KCl (120 mM, pH 7.4) or nomifensine (800 μM) and connected to a microPressure system (Parker Picospritzer III; Aldax). In the DA uptake experiment a single pipette was loaded with 200 μM DA (31). The volume applied was determined and controlled using a stereomicroscope fitted with a reticule in one eyepiece to measure the movement of the meniscus in the micropipette (32). An Ag/AgCl electrode used as a reference electrode was prepared by electroplating an Ag wire in 1 M HCl solution saturated with NaCl for 1 h.

Electrode Implantation and Recording Procedures. Recordings were made simultaneously from electrodes placed bilaterally in the dorsal striatum at 10 d,

3 wk, 5 wk, 8 wk, and 16 wk ($n = 4$ per group) after AAV–α-synuclein injection into the right substantia nigra. Injections of AAV-GFP were used as control ($n = 3$ per group). The animals were anesthetized with urethane (Sigma Aldrich) at a dose of 1.25–1.5 g/kg body weight and placed in a stereotaxic frame. Body temperature was maintained at 37 °C with a constant temperature heating pad connected to a thermostatically controlled water pump (Micro-Temp LT; Cincinnati Sub-Zero). The skull and dura overlying the striatum were bilaterally removed. The Ag/AgCl reference electrode was implanted ≈3 mm into the left hemisphere 4 to 5 mm caudally to bregma. The electrode/micropipette assembly was lowered into the dorsal striatum using the following coordinates calculated from bregma (29): anteroposterior, +1.0 and 0.0 mm; mediolateral, ±3.2 mm; ventral, −4 to −5.0 mm (three sites of measurement with 0.5-mm separation per track). The electrode/micropipette assembly was implanted and left in place at ventral −3.0 mm for 60 min before measurements were initiated. During this time period the anesthesia level and the baseline are stabilized. Once the electrode was in position, four applications of a calibrated volume of KCl were applied by pressure ejection (240–260 nL, 15–20 psi for 0.1–1 s) at 10-min intervals. In each animal extracellular DA levels was monitored after injection of nomifensine (450 nL, 800 μM). Recordings were made simultaneously from the left and the right striatum at the coordinates listed above. The entire measuring procedure lasted for 6 to 7 h starting from the urethane injection.

Signal Parameter Calculations and Statistical Analysis. All parameters of the amperometric data were calculated using FAST analysis version 4.0 for Macintosh (Quanteon). Peak amplitude was calculated as the maximum DA concentration after KCl ejection minus baseline before KCl injection. Reuptake rate is the Michaelis-Menten first-order rate constant (slope of natural log concentration vs. time plot peak maximum) × peak amplitude (μM/s). Linear rise rate (μM/s) was calculated as peak amplitude (μM)/T_{rise} (s), where T_{rise} is the time from KCl injection until peak amplitude is reached. Total amount of extracellular DA is calculated as AUC from KCl injection until the signal has returned to baseline. To reduce variation due to heterogeneity of specific recording sites, an average of the four (repeated releases) × three (depth coordinates) signals in each animal was calculated for all parameters.

Unless stated otherwise, statistical analysis of the amperometric recordings at the five time points was made using two-factor ANOVA, with time point and treatment as factors, followed by Student t test with 95% confidence interval.

Immunohistochemistry. At the end of the recording session the rats were deeply anesthetized with 1.2 mL sodium pentobarbital i.p. (Apoteksbolaget) and perfused through the ascending aorta with 50 mL saline (0.9% wt/vol) at room temperature, followed by 250 mL ice-cold paraformaldehyde (4% wt/vol in 0.1 M PBS). The brains were removed, postfixed for 2 h in 4% paraformaldehyde, cryoprotected overnight in sucrose (25% wt/vol in 0.1 M PBS), and sectioned on a freezing microtome (Leica). Coronal sections were collected in eight series at a thickness of 35 μm.

Stainings was performed on free-floating sections using antibodies raised against TH (rabbit, 1:1,000; Chemicon), VMAT-2 (guinea pig, 1:5,000, Sigma), DAT (rat, 1:500, Chemicon), GFP (rabbit, 1:5,000; Abcam), and human α-synuclein 211 (mouse, 1:10,000; courtesy of Dr. Virginia M. Lee, University of Pennsylvania, Philadelphia, PA). Sections were rinsed three times in potassium-phosphate buffer (KPBS) between each incubation period. All incubation solutions contained 0.25% Triton X-100 in KPBS. The sections were quenched for 10 min in 3% H_2O_2/10% methanol. One hour of preincubation with 5% normal goat serum, normal horse serum, and normal rabbit serum was followed by incubation overnight with the primary antibody in 2% serum at room temperature and incubation with a 1:200 dilution of biotinylated goat anti-rabbit antibody, rabbit anti-rat, or horse anti-mouse (Vector Laboratories), followed by avidin–biotin–peroxidase complex (ABC Elite; Vector Laboratories). Sections were visualized using 3,3-diaminobenzidine as a chromogen, mounted, and coverslipped using DePex mounting medium.

ACKNOWLEDGMENTS. We thank Björn Anzelius and Ulla Jarl for expert technical assistance. This study was supported by grants from the Swedish Research Council (Grant 04X-3874 and the Bagadilico program), the Swedish Foundation for Strategic Research, and the European Union 7th Framework project REPLACES.

1. Cheng H-C, Ulane CM, Burke RE (2010) Clinical progression in Parkinson disease and the neurobiology of axons. *Ann Neurol* 67:715–725.
2. Bernheimer H, Birkmayer W, Hornykiewicz O, Jellinger K, Seitelberger F (1973) Brain dopamine and the syndromes of Parkinson and Huntington. Clinical, morphological and neurochemical correlations. *J Neurol Sci* 20:415–455.
3. Riederer P, Wuketich S (1976) Time course of nigrostriatal degeneration in parkinson's disease. A detailed study of influential factors in human brain amine analysis. *J Neural Transm* 38:277–301.
4. Fearnley JM, Lees AJ (1991) Ageing and Parkinson's disease: Substantia nigra regional selectivity. *Brain* 114:2283–2301.
5. Ma SY, Röyttä M, Rinne JO, Collan Y, Rinne UK (1997) Correlation between neuromorphometry in the substantia nigra and clinical features in Parkinson's disease using disector counts. *J Neurol Sci* 151:83–87.
6. Scherman D, et al. (1989) Striatal dopamine deficiency in Parkinson's disease: Role of aging. *Ann Neurol* 26:551–557.
7. Lotharius J, Brundin P (2002) Impaired dopamine storage resulting from alpha-synuclein mutations may contribute to the pathogenesis of Parkinson's disease. *Hum Mol Genet* 11:2395–2407.
8. Baptista MJ, et al. (2003) Co-ordinate transcriptional regulation of dopamine synthesis genes by alpha-synuclein in human neuroblastoma cell lines. *J Neurochem* 85: 957–968.
9. Larsen KE, et al. (2006) Alpha-synuclein overexpression in PC12 and chromaffin cells impairs catecholamine release by interfering with a late step in exocytosis. *J Neurosci* 26:11915–11922.
10. Nemani VM, et al. (2010) Increased expression of alpha-synuclein reduces neurotransmitter release by inhibiting synaptic vesicle reclustering after endocytosis. *Neuron* 65:66–79.
11. Abeliovich A, et al. (2000) Mice lacking alpha-synuclein display functional deficits in the nigrostriatal dopamine system. *Neuron* 25:239–252.
12. Cabin DE, et al. (2002) Synaptic vesicle depletion correlates with attenuated synaptic responses to prolonged repetitive stimulation in mice lacking alpha-synuclein. *J Neurosci* 22:8797–8807.
13. Chadchankar H, Ihalainen J, Tanila H, Yavich L (2011) Decreased reuptake of dopamine in the dorsal striatum in the absence of α-synuclein. *Brain Res* 1382:37–44.
14. Kirik D, et al. (2002) Parkinson-like neurodegeneration induced by targeted overexpression of alpha-synuclein in the nigrostriatal system. *J Neurosci* 22:2780–2791.
15. Klein RL, King MA, Hamby ME, Meyer EM (2002) Dopaminergic cell loss induced by human A30P alpha-synuclein gene transfer to the rat substantia nigra. *Hum Gene Ther* 13:605–612.
16. Gorbatyuk OS, et al. (2008) The phosphorylation state of Ser-129 in human alpha-synuclein determines neurodegeneration in a rat model of Parkinson disease. *Proc Natl Acad Sci USA* 105:763–768.
17. Chung CY, Koprich JB, Siddiqi H, Isacson O (2009) Dynamic changes in presynaptic and axonal transport proteins combined with striatal neuroinflammation precede dopaminergic neuronal loss in a rat model of AAV alpha-synucleinopathy. *J Neurosci* 29: 3365–3373.
18. Decressac M, Mattsson B, Lundblad M, Weikop P, Björklund A (2011) Progressive neurodegenerative and behavioural changes induced by AAV-mediated overexpression of α-synuclein in midbrain dopamine neurons. *Neurobiol Dis*, 10.1016/j.nbd.2011.12.013.
19. Venda LL, Cragg SJ, Buchman VL, Wade-Martins R (2010) α-Synuclein and dopamine at the crossroads of Parkinson's disease. *Trends Neurosci* 33:559–568.
20. Anwar S, et al. (2011) Functional alterations to the nigrostriatal system in mice lacking all three members of the synuclein family. *J Neurosci* 31:7264–7274.
21. Sidhu A, Wersinger C, Vernier P (2004) alpha-Synuclein regulation of the dopaminergic transporter: A possible role in the pathogenesis of Parkinson's disease. *FEBS Lett* 565:1–5.
22. Oaks AW, Sidhu A (2011) Synuclein modulation of monoamine transporters. *FEBS Lett* 585:1001–1006.
23. Yavich L, et al. (2005) Locomotor activity and evoked dopamine release are reduced in mice overexpressing A30P-mutated human alpha-synuclein. *Neurobiol Dis* 20:303–313.
24. Lam HA, et al. (2011) Elevated tonic extracellular dopamine concentration and altered dopamine modulation of synaptic activity precede dopamine loss in the striatum of mice overexpressing human α-synuclein. *J Neurosci Res* 89:1091–1102.
25. Sidhu A, Wersinger C, Vernier P (2004) Does alpha-synuclein modulate dopaminergic synaptic content and tone at the synapse? *FASEB J* 18:637–647.
26. Volles MJ, et al. (2001) Vesicle permeabilization by protofibrillar alpha-synuclein: Implications for the pathogenesis and treatment of Parkinson's disease. *Biochemistry* 40:7812–7819.
27. Conway KA, Rochet JC, Bieganski RM, Lansbury PT, Jr. (2001) Kinetic stabilization of the alpha-synuclein protofibril by a dopamine-alpha-synuclein adduct. *Science* 294: 1346–1349.
28. Xu J, et al. (2002) Dopamine-dependent neurotoxicity of alpha-synuclein: A mechanism for selective neurodegeneration in Parkinson disease. *Nat Med* 8:600–606.
29. Paxinos G, Watson C (1986) *The Rat Brain in Stereotaxic Coordinates* (Academic Press, New York), 2nd Ed.
30. Hoffman AF, Gerhardt GA (1998) In vivo electrochemical studies of dopamine clearance in the rat substantia nigra: Effects of locally applied uptake inhibitors and unilateral 6-hydroxydopamine lesions. *J Neurochem* 70:179–189.
31. Zahniser NR, Larson GA, Gerhardt GA (1999) In vivo dopamine clearance rate in rat striatum: Regulation by extracellular dopamine concentration and dopamine transporter inhibitors. *J Pharmacol Exp Ther* 289:266–277.
32. Friedemann MN, Gerhardt GA (1992) Regional effects of aging on dopaminergic function in the Fischer-344 rat. *Neurobiol Aging* 13:325–332.